

Holographic entanglement entropies for Schwarzschild and Reisner-Nordström spacetimes

Yuan Sun and Liu Zhao

School of Physics, Nankai University, Tianjin 300071, China

email: sunyuan14@mail.nankai.edu.cn

and lzhao@nankai.edu.cn

Abstract

The holographic entanglement entropies (HEE) associated with four dimensional Schwarzschild and Reisner-Nordström spacetimes are investigated. Unlike the cases of asymptotically AdS spacetimes for which the boundaries are always taken at (timelike) conformal infinities, we take the boundaries at either large but finite radial coordinate (far boundary) or very close to the black hole event horizons (near horizon boundary). The reason for such choices is that such boundaries are similar to the conformal infinity of AdS spacetime in that they are all timelike, so that there may be some hope to define dual systems with ordinary time evolution on such boundaries. Our results indicate that, in the case of far boundaries, the leading order contribution to the HEEs come from the background Minkowski spacetime, however, the next to leading order contribution which arises from the presence of the black holes is always proportional to the black hole mass, which constitutes a version of the first law of the HEE for asymptotically flat spacetimes, and the higher order contributions are always negligibly small. In the case of near horizon boundaries, the leading order contribution to the HEE is always proportional to the area of the black hole event horizon, and the case of extremal RN black hole is distinguished from the cases of non-extremal black holes in that the minimal surface defining the HEE is completely immersed inside the boundary up to the second order in the perturbative expansion.

1 Introduction

Holography has now been widely accepted as one of the fundamental properties of relativistic gravitational theories, largely due to the discovery of AdS/CFT duality [1]. In its preliminary form, holographic principle was originally proposed by 't Hooft [2] and Susskind [3] respectively, which simply states that the microscopic degrees of freedom of

a black hole reside solely on its horizon surface. In AdS/CFT, however, the holographic surface is promoted to the boundary at conformal infinity. Certainly this promotion has important significance and physical consequences. Since the boundary at conformal infinity for asymptotically AdS spacetime is a timelike hypersurface, the dual theory on the boundary behaves as a field theory defined on a co-dimension one spacetime. In particular, it is a theory sitting at the fixed point of the renormalization group, i.e. a conformal field theory. One can use the holographic duality to study the properties of the dual theory by looking at the corresponding features in the bulk or vice versa.

Despite its great success, one should keep in mind that AdS/CFT is not the full story for holography. The study of holographic properties of non-asymptotically AdS spacetimes have not been promoted to the same level of depth. One reason for this lies in that, for non-asymptotically AdS spacetimes, the boundary at conformal infinity is usually not a timelike hypersurface and hence it is difficult to define the dual theory as a normal field theory. To this end let us mention that for asymptotically flat spacetimes, the conformal infinity is always lightlike, which is very different from a timelike hypersurface. There are other reasons, for instance, even if one can manage to define a dual theory, it will be usually nonlocal [4] and lacks physical interests.

Even though there are various difficulties while considering the holographic properties of non-asymptotically AdS spacetimes, they can never be enough to serve as a mind stopper. Various attempts have been practiced towards this problem [4–10]. Among them, the holographic entanglement entropy (HEE) seems to be particularly suitable for tackling this problem. Roughly speaking, the HEE is a shortcut for calculating the entanglement entropy of a subsystem in the dual theory. When the bulk theory is Einstein gravity, Ryu and Takayanagi conjectured that the entanglement entropy of a subsystem on the boundary is identical to the area (divided by $4G$) of a minimal surface which takes the entanglement surface as its own boundary [11, 12]. This conjecture has been proven in [13], and also generalized to time-dependent background [14] and higher derivative gravity [15].

Since RT formula involves the minimal surface, it is important to analyze such minimal surfaces in various asymptotically AdS spacetime with black hole in the bulk or time-dependent background, for instance in [16, 17]. Extremal surfaces are also analyzed in de Sitter spacetime [18, 19]. In this paper, we shall take Ryu-Takayanagi conjecture as the definition of HEE in asymptotically flat spacetimes [4]. More concretely, we shall study the HEE in four dimensional Schwarzschild and Reissner-Nordström (RN) spacetimes and analyze its dependence on various impacting parameters. To avoid getting only divergent results, we do not put the boundary at conformal infinity. Instead, we take the boundary at some finite radial position which is either very far from the black hole horizon or is very close to the horizon. Such boundary hypersurfaces are all timelike, and therefore there leaves room for defining normal dual field theories on such hypersurfaces. However, remember that the boundary hypersurfaces we take are not sitting at the renormalization group fixed point, so even there exist normal dual field theories, these will not be conformal. Such theories may just be some off critical theories.

The rest of this paper is organized as follows. In Section 2, we study the HEE in Schwarzschild and RN spacetimes with far boundaries. It will be shown that the behavior of the HEE for both spacetimes are quite similar. The difference begins to show up only at the second order in the perturbative expansion, which is negligibly small. In Section 3, we study the same problem but with the far boundaries replaced by near horizon ones. The HEE behaves differently for the case of extremal RN spacetime in contrast to the cases of Schwarzschild and non-extremal RN spacetimes. The HEEs in all cases will be calculated up to the second order in the perturbative expansion and will be cross checked by numerical procedures. In the last section, Section 4, we summarize some of the interesting results obtained in this paper.

2 HEE in Schwarzschild and RN spacetimes – far boundary

In this section, we shall study the HEE in Schwarzschild and RN spacetimes with the dual theory defined on a boundary located at large but finite radial coordinate $r = r_\infty$. The bulk theory is assumed to be Einstein gravity and the spacetime metric takes the well known form

$$ds^2 = -A(r)dt^2 + B(r)dr^2 + r^2(d\theta^2 + \sin^2\theta d\varphi^2),$$

$$A(r) = B(r)^{-1} = 1 - \frac{2M}{r} + \frac{Q^2}{r^2}. \quad (1)$$

When both of the parameters M and Q equal to zero, the metric becomes that of the Minkowski spacetime. When $M \neq 0$ but $Q = 0$, the metric corresponds to Schwarzschild spacetime. And when both Q and M are nonzero, the metric corresponds to RN spacetime. With either $M \neq 0$ or both M and Q are nonzero, we can think of the contributions of the terms involving M and/or Q as perturbations at large enough radial distances.

In this section, we take the boundary hypersurface at $r = r_\infty$ with r_∞ very large but still finite. The entanglement surface will be taken to be a circle characterized by $\theta = \theta_0$, and the minimal surface which takes the entanglement surface as its boundary can be described by the radial coordinate r as a function of θ , i.e. $r = r(\theta)$, which is to be determined via the minimization of the area function

$$\mathcal{A} = 2\pi \int_0^{\theta_0} d\theta r \sin\theta \sqrt{B(r) \left(\frac{dr}{d\theta}\right)^2 + r^2}, \quad (2)$$

with the boundary condition $r(\theta_0) = r_\infty$. Once the above variational problem is solved, the HEE will be given by the Ryu-Takayanagi formula

$$S = \frac{\mathcal{A}}{4G}. \quad (3)$$

First let us consider the HEE in the Minkowski background. In this case, we have $B = 1$ and the minimal surface is simply a flat disk with equation $z_0 = r_\infty \cos \theta_0 = r \cos \theta$. This surface has area $\pi r_\infty^2 \sin^2 \theta_0$, hence the HEE is [4]

$$S_0 = \frac{\pi r_\infty^2 \sin^2 \theta_0}{4G} = \frac{\pi z_0^2 \tan^2 \theta_0}{4G}. \quad (4)$$

Now let us return to the case with generic M and Q . For simplicity we denote $x = \cos \theta$. Then the area formula (39) can be rewritten as

$$\mathcal{A} = \int_{x_0}^1 dx L = 2\pi \int_{x_0}^1 dx r \sqrt{B(r)(1-x^2)r'^2 + r^2}, \quad (5)$$

where $x_0 = \cos \theta_0$ and the prime denotes derivative with respect to x . Variation of (5) with respect to $r(x)$ yields the equation

$$(x^2 - 1) \left[2Br^2r'' - 2xB^2r'^3 + \left(r \frac{dB}{dr} - 6B \right) rr'^2 \right] + 4xBr^2r' + 4r^3 = 0. \quad (6)$$

When $B[r(x)] = 1$, one can check that $r = z_0/x$ is a solution. The equation (6) is highly nonlinear. In order to get a nontrivial solution with nonzero M and Q , let us expand $B[r(x)]$ and $r(x)$ into formal series,

$$B[r(x)] = 1 - \sum_{n=1} f_n(x) \epsilon^n, \quad (7)$$

$$r(x) = \frac{z_0}{x} + \sum_{n=1} r_n(x) \epsilon^n, \quad (8)$$

where $\epsilon = \frac{M}{r_\infty}$ is a small dimensionless constant and all terms in positive powers of ϵ in eqs. (7) and (8) represent modifications arising from the presence of black hole. The absence of $O(\epsilon^0)$ term in (8) can be understood from the background solution $B[r(x)] = 1, r(x) = z_0/x$. Using the full form of $B[r(x)]$ presented in (1), it is not difficult to get

$$f_1(x) = -\frac{2r_\infty x}{z_0}, \quad f_2(x) = \frac{r_\infty x^2 [(\xi^2 - 4)r_\infty + 2r_1(x)]}{z_0^2}, \quad \dots \quad (9)$$

where $\xi = Q/M$ is the charge to mass ratio. For Schwarzschild spacetime, $\xi = 0$. For RN spacetime, $\xi \neq 0$, wherein $0 < |\xi| < 1$ represents a non-extremal black hole spacetime, $|\xi| = 1$ represents an extremal spacetime, and $|\xi| > 1$ corresponds to a spacetime with a naked singularity.

In the following, we shall use the above expansion to get approximate solutions to the equation (6) up to the second order in ϵ and evaluate the corresponding modifications to the HEE. Similar procedures have been applied in [20] wherein the metric perturbation of HEE in global AdS coordinate is studied, and also in [22], where the time dependence of holographic entanglement complexity is analyzed.

2.1 First order

To the first order in ϵ , eq. (6) becomes

$$r_1'' + \frac{5x^2 - 3}{x^3 - x} r_1' + \frac{3x^2 - 1}{x^4 - x^2} r_1 = \frac{r_\infty(3x^2 + 1)}{x^4 - x^2}. \quad (10)$$

With f_1 provided as a known function, eq. (10) is a second order linear inhomogeneous differential equation in $r_1(x)$. It is known that for generic second order linear inhomogeneous differential equations of the form

$$r_1'' + P(x)r_1' + Q(x)r_1 = G(x), \quad (11)$$

the general solution can be written as

$$r_1(x) = c_1 u_1(x) + c_2 u_2(x) + \int^x dy \frac{(u_1(y)u_2(x) - u_1(x)u_2(y))G(y)}{W(y)}, \quad (12)$$

where u_1 and u_2 are solutions for the homogeneous equation

$$r_1'' + P(x)r_1' + Q(x)r_1 = 0, \quad (13)$$

and $W = u_1 u_2' - u_1' u_2$ is the Wronskian of the solutions u_1 and u_2 .

For eq.(10), we can easily get

$$u_1(x) = \frac{1}{x}, \quad u_2 = \frac{2 \ln x - \ln(1 - x^2)}{2x}, \quad (14)$$

and hence

$$W(x) = \frac{1}{x^3 - x^5}. \quad (15)$$

Inserting $W(x)$ and

$$G(x) = \frac{r_\infty(3x^2 + 1)}{x^4 - x^2} \quad (16)$$

into (12), we get

$$r_1(x) = \frac{c_1}{x} + c_2 \frac{2 \ln x - \ln(1 - x^2)}{2x} + r_\infty \left(1 + \frac{\ln(1 - x)}{x} - \frac{\ln(1 + x)}{x} \right). \quad (17)$$

Since $x = \cos \theta \in [\cos \theta_0, 1]$, the terms containing $\ln(1 - x)$ must be cancelled to avoid divergence, which is used to determine $c_2 = 2r_\infty$. c_1 can be fixed by the boundary condition $r_1(x_0) = 0$, which results in

$$c_1 = r_\infty [-x_0 - 2 \ln x_0 + 2 \ln(1 + x_0)]. \quad (18)$$

Finally the first order contribution to $r(x)$ is

$$r_1(x) = \frac{r_\infty}{x} \left[(x - x_0) + 2 \log \left(\frac{x}{x_0} \right) + 2 \log \left(\frac{x_0 + 1}{x + 1} \right) \right]. \quad (19)$$

Notice that r_1 given above diverges when $x = 0$ (i.e. $\theta = \pi/2$), therefore it is necessary to restrict $\theta_0 < \pi/2$, so that $x = 0$ can never be approached. This is a limitation of the perturbative expansion in the case of far boundaries. The same limitation also appears in the case of AdS background [20].

In order to evaluate the first order modification to the HEE, let us expand the integrand L in (5) to the first order in ϵ ,

$$L = L_0 + L_1\epsilon + \dots, \quad (20)$$

so that (5) becomes

$$\mathcal{A} = \mathcal{A}_0 + \mathcal{A}_1 + \dots, \quad (21)$$

with

$$\begin{aligned} \mathcal{A}_0 &= \int_{x_0}^1 dx L_0 = \int_{x_0}^1 dx \frac{2\pi z_0^2}{x^3} = \pi z_0^2 \left(\frac{1}{x_0} - 1 \right), \\ \mathcal{A}_1 &= \epsilon \int_{x_0}^1 dx L_1 = \frac{M}{r_\infty} \int_{x_0}^1 dx \frac{4\pi r_\infty z_0}{x^3} \left[2x - x_0 - 1 + 2 \log \left(\frac{x}{x_0} \right) + 2 \log \left(\frac{x_0 + 1}{x + 1} \right) \right] \\ &= 2\pi M(1 - x_0)^2 r_\infty. \end{aligned} \quad (22) \quad (23)$$

It is not surprising that replacing \mathcal{A} with \mathcal{A}_0 in (3) would yield the HEE (4) at the background level. Similarly, replacing \mathcal{A} with \mathcal{A}_1 in (3) yields the first order modification to the HEE,

$$S_1 = \frac{\pi M(1 - x_0)^2}{2G} r_\infty. \quad (24)$$

Since we assume r_∞ to be very large and $S_0 \propto r_\infty^2$, $S_1 \propto r_\infty$, we can safely regard S_1 to be a “small” modification to S_0 . An important point to observe is that

$$\delta S \equiv S - S_0 \simeq S_1 = \frac{\pi r_\infty(1 - x_0)^2}{2G} M, \quad (25)$$

i.e. the small modification to the HEE is proportional to the black hole mass. This behavior is similar to the case of HEE associated with black holes in AdS backgrounds [21]. In the latter case, the result $\delta S \propto M$ is known as the first law of HEE. Another point to observe lies in that S_1 is independent of the charge Q , so that it can not distinguish the cases of Schwarzschild and RN black holes. This is also not surprising because we are now considering the far boundaries, and the charge term in (1) plays as the second order modification in the far end. To observe the contribution of the charge parameter, we have to move on to the second order.

2.2 Second order

At the second order, eq.(6) takes the form

$$r_2'' + \frac{5x^2 - 3}{x^3 - x} r_2' + \frac{3x^2 - 1}{x^4 - x^2} r_2 = G_2(x), \quad (26)$$

where the homogeneous part takes the same form as that of the first order equation (10), thus the solutions of the homogeneous equation remain unchanged. The inhomogeneous term $G_2(x)$ takes the value

$$G_2(x) = \frac{2r_\infty^2 [(\xi^2 - 1)x^3 - 3x + 4]}{z_0 x^2 (1 - x^2)}. \quad (27)$$

The solution of eq.(26) can be written as

$$r_2(x) = c_3 u_1(x) + c_4 u_2(x) + u(x), \quad (28)$$

where u_1, u_2 are given in (14), and

$$\begin{aligned} u(x) &\equiv \int^x dy \frac{(u_1(y)u_2(x) - u_1(x)u_2(y))G_2(y)}{W(y)} \\ &= -\frac{r_\infty^2 ((\xi^2 - 1)x^2 + (\xi^2 + 9)\log(1 - x) + (\xi^2 - 23)\log(x + 1))}{4xz_0}. \end{aligned}$$

Similar to the case discussed in the previous subsection, the integration constant c_4 can be determined by the cancellation of the term involving $\ln(1 - x)$, and the boundary condition $r_2(x_0) = 0$ fixes c_3 ,

$$c_3 = \frac{r_\infty^2}{4z_0} [(\xi^2 - 1)x_0^2 + 2(\xi^2 + 9)\log x_0 - 32\log(1 + x)], \quad (29)$$

$$c_4 = -\frac{r_\infty^2(\xi^2 + 9)}{2z_0}. \quad (30)$$

Thus we get the final expression for $r_2(x)$,

$$r_2(x) = \frac{r_\infty^2}{4z_0 x} \left[(1 - \xi^2)(x^2 - x_0^2) + 2(\xi^2 + 9)\log\left(\frac{x_0}{x}\right) + 32\log\left(\frac{1 + x}{1 + x_0}\right) \right]. \quad (31)$$

To obtain the second order modification to the HEE, we need to expand the area \mathcal{A} and the integrand L in (5) up to the second order,

$$L = L_0 + L_1\epsilon + L_2\epsilon^2 + \dots, \quad (32)$$

$$\mathcal{A} = \mathcal{A}_0 + \mathcal{A}_1 + \mathcal{A}_2 + \dots. \quad (33)$$

Omitting the very complicated expression for L_2 , we present directly the final result for $S_2 \equiv \frac{\mathcal{A}_2}{4G} = \frac{\epsilon^2}{4G} \int_{x_0}^1 dx L_2$:

$$S_2 = \frac{\pi}{8G} \left\{ \left[(1 - x_0)(x_0 - 7) + 2\log x_0 + 16\log\left(\frac{2}{1 + x_0}\right) \right] M^2 + [1 - x_0^2 + 2\log x_0] Q^2 \right\}. \quad (34)$$

It can be seen explicitly that the charge begins to contribute at this order, but since $S_2/S_1 \sim O(\epsilon)$, such contribution is always negligibly small. As a consequence, the first law for the HEE

$$\delta S = S - S_0 \propto M \quad (35)$$

holds very well even if we calculate S up to the second order.

3 HEE in Schwarzschild and RN spacetimes – near horizon

The study of HEE with entangling surface located on the far boundary indicates that there is no significant difference between the cases of Schwarzschild and RN spacetimes. This is of course just an illusion stemming from the particular choice of boundary at large r_∞ . In this section, we shall study the opposite choice, i.e. near horizon boundaries. For such boundaries, the differences between the HEEs for Schwarzschild, non-extremal RN and extremal RN spacetimes will become more transparent.

3.1 Schwarzschild

First we consider the case of Schwarzschild spacetime by setting $Q = 0$ in (1). In the near horizon limit, it is convenient to introduce a new radial coordinate

$$\rho = \sqrt{r - r_+}, \quad (r_+ = 2M) \quad (36)$$

after which the metric on the constant t hypersurface becomes

$$ds^2 = 4g(\rho)d\rho^2 + g(\rho)^2(d\theta^2 + \sin^2\theta d\varphi^2), \quad (37)$$

where $g(\rho) = r_+ + \rho^2$. In this new coordinate, the black hole event horizon is located at $\rho = 0$.

Now let us take a near horizon boundary at $\rho = \rho_0$ with $\epsilon \equiv \rho_0/\sqrt{r_+} \ll 1$. Once again, the one dimensional circle characterized by $\theta = \theta_0$ is taken as the entangling surface. The two dimensional minimal surface which takes the above circle as its boundary possesses an induced metric

$$ds^2 = \left[4g(\rho) \left(\frac{d\rho}{d\theta} \right)^2 + g(\rho)^2 \right] d\theta^2 + [g(\rho) \sin\theta]^2 d\varphi^2, \quad (38)$$

where $\rho = \rho(\theta)$ is to be determined by minimizing the surface area

$$\mathcal{A} = \int_{x_0}^1 dx d\varphi L = 2\pi \int_{x_0}^1 dx g(\rho) [4g(\rho)(1 - x^2)\rho'^2 + g(\rho)^2]^{1/2}, \quad (39)$$

Notice that we have made a coordinate change $\theta \rightarrow x = \cos\theta$ in eq.(39) just like in the last subsection, and the prime denotes derivative with respect to x .

The variation of eq.(39) yields

$$2g(x^2 - 1)\rho'' + 8x(1 - x^2)\rho'^3 + 5(1 - x^2)\frac{dg}{d\rho}\rho'^2 + 4gx\rho' + g\frac{dg}{d\rho} = 0. \quad (40)$$

Direct analytical solution to (40) seems to be very difficult to find. Therefore, we would like to find the minimal surface perturbatively following a similar procedure as we have done in the case of far boundaries.

By observing eq.(39), one sees that any surface anchored on the circle at $\rho = \rho_0, \theta = \theta_0$ and extended into the bulk with $\rho > \rho_0$ will have an area greater than that of the surface lies along $\rho = \rho_0$ with the same boundary. In other words, if there exists a minimal surface anchored on the above circle, it must lie in the region $\rho < \rho_0$. Thus the expansion of $\rho(x)$ must start from the first order in ϵ ,

$$\rho(x) = \rho_1(x)\epsilon + \rho_2(x)\epsilon^2 + \cdots, \quad (41)$$

and the boundary condition $\rho(x_0) = \rho_0$ becomes

$$\rho_1(x_0) = \sqrt{r_+}, \quad \rho_2(x_0) = 0. \quad (42)$$

Substituting eq.(41) into (40) and expanding to the first order in ϵ , one gets

$$(x^2 - 1)\rho_1'' + 2x\rho_1' + \rho_1 = 0. \quad (43)$$

This is a special case of the Legendre equation. The solution which is regular at $x = 1$ and satisfies the boundary condition (42) reads

$$\rho_1(x) = c_1 P_\nu(x), \quad \nu = -e^{-i\pi/3}, \quad c_1 = \frac{\sqrt{r_+}}{P_\nu(x_0)}, \quad (44)$$

where $P_\nu(x)$ is the Legendre polynomial of the first kind. Expanding to the second order in ϵ , the equation for ρ_2 follows,

$$(x^2 - 1)\rho_2'' + 2x\rho_2' + \rho_2 = 0. \quad (45)$$

This equation takes the same form as (43). Thus the solution can be written as

$$\rho(x) = c_2 P_\nu(x), \quad \nu = -e^{-i\pi/3}, \quad (46)$$

and the boundary condition $\rho_2(x_0) = 0$ requires $c_2 = 0$, which sets $\rho_2(x) = 0$.

Inserting eq.(41) into the integrand L in (39), we get

$$L = 2\pi r_+^2 + 4\pi r_+[(1 - x^2)\rho_1'^2 + \rho_1^2]\epsilon^2 + \cdots. \quad (47)$$

Substituting back into (39) and expand \mathcal{A} accordingly,

$$\mathcal{A} = \mathcal{A}_0 + \mathcal{A}_1 + \mathcal{A}_2 + \cdots, \quad (48)$$

we will have

$$\mathcal{A}_0 = 2\pi r_+^2(1 - x_0), \quad \mathcal{A}_1 = 0, \quad (49)$$

and

$$\mathcal{A}_2 = \frac{4\pi r_+ \rho_0^2}{(P_\nu(x_0))^2} \int_{x_0}^1 dx \left[(1 - x^2) \left(\frac{dP_\nu(x)}{dx} \right)^2 + (P_\nu(x))^2 \right]. \quad (50)$$

The last integration cannot be worked out analytically, however it is easy to get the numerical result. It turns out that for all $-1 < x_0 < 1$, \mathcal{A}_2 is finite and is less than 1 in units of $4\pi r_+ \rho_0^2$. Fig.1 gives the plot of $\mathcal{A}_2/(4\pi r_+ \rho_0^2)$ versus x_0 . Since $4\pi r_+ \rho_0^2$ is roughly $\epsilon^2 \mathcal{A}_0$, we can see that the HEE associated with Schwarzschild spacetime with a near horizon boundary is almost precisely given by the zeroth order contribution. In particular, the HEE equals the Beckenstein-Hawking entropy for the black hole when $x_0 = -1$, i.e. $\theta_0 = \pi$. Let us remark that there is no problem of divergence in the case of near horizon boundaries.

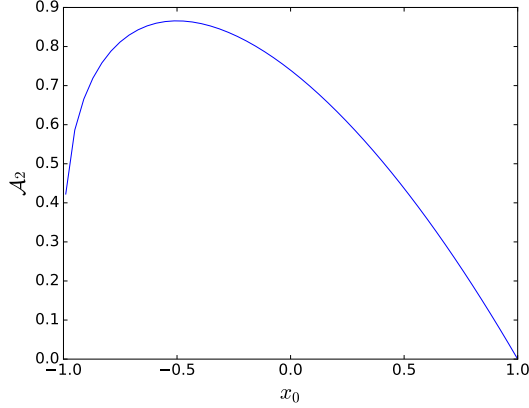


Figure 1: \mathcal{A}_2 versus x_0 , in units of $4\pi r_+ \rho_0^2$

3.2 Non-extremal RN

Let us now turn our attention to the case of non-extremal RN black hole spacetime with a near horizon boundary.

For non-extremal RN black hole spacetime, the functions $A(r)$ and $B(r)$ in (1) can be written in a factorized form,

$$A(r) = B(r)^{-1} = \frac{(r - r_-)(r - r_+)}{r^2}, \quad r_{\pm} = M \pm \sqrt{M^2 - Q^2}. \quad (51)$$

In the near horizon limit, making the coordinate transformation $r \rightarrow \rho$ with $r = r_+ + \rho^2$, the metric on a constant t -slice becomes

$$ds^2 = f(\rho)d\rho^2 + g(\rho)^2(d\theta^2 + \sin^2 \theta d\varphi^2), \quad (52)$$

where

$$g(\rho) = r_+ + \rho^2, \quad f(\rho) = \frac{4(\rho^2 + r_+)^2}{\rho^2 + r_+ - r_-}. \quad (53)$$

The induced metric on a co-dimension 2 minimal surface is

$$d\hat{s}^2 = [f(\rho)(1 - x^2)\rho'^2 + g(\rho)^2] d\theta^2 + g(\rho)^2 \sin^2 \theta d\varphi^2, \quad (54)$$

where again $x = \cos \theta$ and primes denote derivatives with respect to x . The area functional is then

$$\mathcal{A} = \int dx d\varphi L = 2\pi \int dx g(\rho) [f(\rho)(1 - x^2)\rho'^2 + g(\rho)^2]^{1/2}, \quad (55)$$

and the minimization condition yields the following differential equation:

$$(1 - x^2) \left[-2fg^2\rho'' + 2f^2x\rho'^3 - \left(\frac{df}{d\rho}g^2 - 6fg\frac{dg}{d\rho} \right) \rho'^2 \right] + 4fg^2x\rho' + 4g^3\frac{dg}{d\rho} = 0. \quad (56)$$

Let us again take the small parameter $\epsilon \equiv \rho_0/\sqrt{r_+} \ll 1$ and make the expansion

$$\rho(x) = \rho_1\epsilon + \rho_2\epsilon^2 + \dots \quad (57)$$

In the first order, eq.(56) can be reduced into

$$(x^2 - 1)\rho_1'' + 2x\rho_1' + \frac{r_+ - r_-}{r_+}\rho_1 = 0. \quad (58)$$

Once again, we get a specific Legendre equation and the general solution reads

$$\rho_1(x) = c_1 P_\nu(x) + c_2 Q_\nu(x), \quad \nu = \sqrt{\frac{r_-}{r_+} - \frac{3}{4}} - \frac{1}{2}. \quad (59)$$

Here $Q_\nu(x)$ is the Legendre polynomial of the second kind, and $0 < r_-/r_+ < 1$. The solution regular at $x = 1$ for generic choice of r_\pm is

$$\rho_1(x) = c_1 P_\nu(x), \quad c_1 = \frac{\sqrt{r_+}}{P_\nu(x_0)}, \quad (60)$$

where c_1 is determined by the boundary condition $\rho_1(x_0)\epsilon = \rho_0$.

The equation at the next order takes the same form as that for ρ_1 , i.e.

$$(x^2 - 1)\rho_2'' + 2x\rho_2' + \frac{r_+ - r_-}{r_+}\rho_2 = 0. \quad (61)$$

Then the the boundary condition $\rho_2(x_0) = 0$ forces $\rho_2(x) = 0$, just as in the Schwarzschild case.

Now let us expand the integrand L in (54) up to the second order in ϵ ,

$$L = 2\pi r_+^2 + \frac{4\pi r_+^2}{r_+ - r_-} \left((1 - x^2)\rho_1'^2 + \frac{r_+ - r_-}{r_+}\rho_1^2 \right) \epsilon^2 + \dots \quad (62)$$

Then the area of the minimal surface is

$$\begin{aligned} \mathcal{A} &= 2\pi(1 - x_0)r_+^2 + \frac{4\pi r_+^2}{r_+ - r_-} \int_{x_0}^1 dx \left((1 - x^2)\rho_1'^2 + \frac{r_+ - r_-}{r_+}\rho_1^2 \right) \epsilon^2 + \dots \\ &= 2\pi(1 - x_0)r_+^2 + \frac{4\pi r_+ \rho_0^2}{r_+ - r_-} \int_{x_0}^1 dx \left((1 - x^2)\rho_1'^2 + \frac{r_+ - r_-}{r_+}\rho_1^2 \right) + \dots \end{aligned} \quad (63)$$

When $r_- = 0$, this reduces to the corresponding result for the Schwarzschild case. Note, however, that the second order term contains $r_+ - r_-$ in the denominator, therefore this result is not applicable to the case of extremal RN black hole (i.e. the $r_+ = r_-$ case).

3.3 Extremal RN

For extremal RN black hole spacetime, (51) becomes

$$A(r) = B(r)^{-1} = \frac{(r - r_+)^2}{r^2}, \quad r_+ = M. \quad (64)$$

Making a coordinate change $r \rightarrow \rho$ with $r = r_+ + \rho^2$, the metric on the constant t -slice of the spacetime reads

$$ds^2 = f(\rho)d\rho^2 + g(\rho)^2(d\theta^2 + \sin^2\theta d\varphi^2), \quad (65)$$

with

$$g(\rho) = r_+ + \rho^2, \quad f(\rho) = \frac{4(\rho^2 + r_+)^2}{\rho^2}. \quad (66)$$

Formally, this metric is identical to (52), the only difference lies in that we have now a different function $f(\rho)$ in the first term on the right hand side. Repeating the process as in (54)-(56) and carrying out the expansion (57), we can get a very complicated equation with a denominator of order $O(\epsilon)$. Discarding this denominator and looking only at the numerator, we can get, at the leading order $O(\epsilon^0)$, the following equation for $\rho_1(x)$,

$$2x\rho_1^2\rho_1' + (1 - x^2)(-\rho_1^2\rho_1'' + 4x\rho_1'^3 + \rho_1\rho_1'^2) = 0. \quad (67)$$

This is a nonlinear homogeneous differential equation in which every term is cubic in the function $\rho_1(x)$. This equation can have many analytical solutions, but the only solution which satisfies the boundary condition $\rho_1(x_0)\epsilon = \rho_0$ and is regular at $x = 1$ is a constant solution

$$\rho_1(x) = \rho_0/\epsilon = \sqrt{r_+}. \quad (68)$$

We can evaluate the numerator of (56) to the next few orders in ϵ and find that the only solution for $\rho_2(x)$ which obeys the boundary condition $\rho_2(x_0)\epsilon^2 = 0$ is simply $\rho_2(x) = 0$. Thus we have $\rho(x) = \rho_1(x)\epsilon = \rho_0$, i.e. the minimal surface is completely immersed inside the boundary surface. It should be remarked that $\rho = \text{const}$ is *not* an exact solution of the original non-expanded equation (56), so there must be some non-constant contributions to $\rho(x)$ at higher orders. However, up to the second order in ϵ , only constant solution is permitted by the boundary conditions.

Finally, we come to evaluate the area of the minimal surface using (55). Since now $\rho'(x) = 0$, we have

$$\mathcal{A} = 2\pi \int_{x_0}^1 dx g(\rho)^2 = 2\pi(1 - x_0)r_B^2, \quad (69)$$

where $r_B = r_+ + \rho_0^2$ is the radius of the boundary surface.

To verify the correctness of the perturbative procedures used in this section, we also studied the numerical solution to the equation (56) for both the non-extremal and extremal cases. The results are presented in Fig.2 and Fig.3. These figures are created

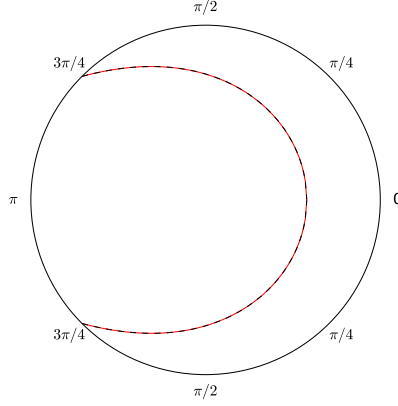


Figure 2: The minimal surface in the case of a non-extremal RN black hole with a near horizon boundary. The red curve is the numerical solution of (56). The dashed black curve is the perturbative solution (57). The parameters are taken as: $\theta_0 = 3\pi/4$, $\rho_0 = 0.02$, $r_+ = 0.9$, $r_- = 0.6$.

in the (ρ, θ) coordinates, with the φ coordinate omitted. The black hole event horizons are located at $\rho = 0$ in such coordinates and are not demonstrated.

Fig.2 corresponds to the case of a non-extremal RN black hole with a near horizon boundary (shown as the outer-most circle). The entangling surface is characterized by the single parameter $\theta_0 = 4\pi/3$. The other parameters are $\rho_0 = 0.02$, $\theta_0 = -3\pi/4$, $r_+ = 0.9$, $r_- = 0.6$.

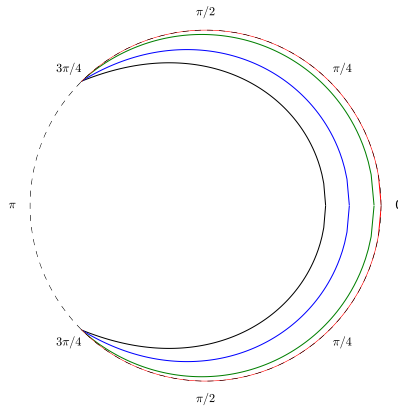


Figure 3: The minimal surfaces of several RN black holes with near horizon boundaries. Different curves correspond to different choices of the parameter r_- : $r_- = 0.7$ (black), $r_- = 0.8$ (blue), $r_- = 0.88$ (green), $r_- = 0.9$ (red). The last case corresponds to extremal black hole, with numerical (red) and perturbative (dashed) results in good agreements.

Fig.3 gives the plot of minimal surfaces for several different RN black hole space-

times. The parameters θ_0, ρ_0 and r_+ are identical to the case of Fig.2, however several different values of r_- are taken in order to indicate the change of minimal surface with respect to this parameter. Among these, the largest choice $r_- = 0.9$ corresponds to the case of an extremal black hole. It can be seen that in both figures the perturbative results are in very good agreements with the numerical solutions.

4 Conclusion

In this paper, we studied the HEE associated with two asymptotically flat spacetimes, i.e. Schwarzschild and RN spacetimes, with boundaries taken either at large but finite radial distances or close to the black hole event horizon. Here we summarize some of the interesting results:

- At the far end, the HEE for both spacetimes are identical at the leading and the next to leading orders. The leading order contribution is actually the HEE associated with the background Minkowski spacetime, so the majority of the true contribution from the black holes comes in the next to leading order. It is shown that the next to leading order contribution to the HEE is always proportional to the black hole mass, regardless whether we are considering Schwarzschild or RN spacetimes. This gives a version of the first law of HEE for asymptotically flat spacetimes.
- Still at the far end, the case of RN spacetime begins to show off at the next to next to leading order $O(\epsilon^2)$. We have shown that there is an extra term which is proportional to Q^2 for the RN case. There are no conceivable differences between the cases for extremal and non-extremal RN black hole spacetimes.
- In the near horizon case, the HEE for Schwarzschild and non-extremal RN spacetimes are also quite similar: at the leading order, the HEE is proportional to the horizon area, and it actually equals to the horizon area if the subsystem is defined on the whole spherical boundary with a single point removed. The next to leading order contributions always vanish.
- Also in the near horizon case, the HEE for extremal and non-extremal RN spacetime behave quite differently. For the non-extremal case, the minimal surface anchored on the entangling surface on the boundary bends inwards, and hence the HEE is smaller than the area of the subsystem on the boundary divided by $4G$. However, for the extremal case, the minimal surface is completely immersed inside the boundary, up to the second order in the perturbative expansion. Therefore the HEE is equal to the area of the subsystem on the boundary divided by $4G$ on the same level of approximation.

Of course, the HEE associated with asymptotically flat spacetime is a subtle and relatively new subject and deserves further study. The content presented in this work should only be considered as initiating rather than closing this new area of study.

Acknowledgment

This work is supported by the National Natural Science Foundation of China under the grant No. 11575088.

References

- [1] J. M. Maldacena, “The Large N limit of superconformal field theories and supergravity,” *Int. J. Theor. Phys.* **38**, 1113 (1999) [*Adv. Theor. Math. Phys.* **2**, 231 (1998)] doi:10.1023/A:1026654312961 [hep-th/9711200].
- [2] G. ’t Hooft, “Dimensional reduction in quantum gravity,” *Salamfest 1993*:0284-296 [gr-qc/9310026].
- [3] L. Susskind, “The World as a hologram,” *J. Math. Phys.* **36**, 6377 (1995) doi:10.1063/1.531249 [hep-th/9409089].
- [4] W. Li and T. Takayanagi, “Holography and Entanglement in Flat Spacetime,” *Phys. Rev. Lett.* **106**, 141301 (2011) doi:10.1103/PhysRevLett.106.141301 [arXiv:1010.3700 [hep-th]].
- [5] R. Bousso, “Holography in general space-times,” *JHEP* **9906**, 028 (1999) doi:10.1088/1126-6708/1999/06/028 [hep-th/9906022].
- [6] A. Strominger, “The dS / CFT correspondence,” *JHEP* **0110**, 034 (2001) doi:10.1088/1126-6708/2001/10/034 [hep-th/0106113].
- [7] F. Sanches and S. J. Weinberg, “Holographic entanglement entropy conjecture for general spacetimes,” *Phys. Rev. D* **94**, no. 8, 084034 (2016) doi:10.1103/PhysRevD.94.084034 [arXiv:1603.05250 [hep-th]].
- [8] Y. Nomura, N. Salzetta, F. Sanches and S. J. Weinberg, “Toward a Holographic Theory for General Spacetimes,” arXiv:1611.02702 [hep-th].
- [9] A. Bagchi, R. Basu, D. Grumiller and M. Riegler, “Entanglement entropy in Galilean conformal field theories and flat holography,” *Phys. Rev. Lett.* **114**, no. 11, 111602 (2015) doi:10.1103/PhysRevLett.114.111602 [arXiv:1410.4089 [hep-th]].
- [10] A. Bagchi, R. Basu, A. Kakkar and A. Mehra, “Flat Holography: Aspects of the dual field theory,” arXiv:1609.06203 [hep-th].
- [11] S. Ryu and T. Takayanagi, “Holographic derivation of entanglement entropy from AdS/CFT,” *Phys. Rev. Lett.* **96**, 181602 (2006) doi:10.1103/PhysRevLett.96.181602 [hep-th/0603001].
- [12] S. Ryu and T. Takayanagi, “Aspects of Holographic Entanglement Entropy,” *JHEP* **0608**, 045 (2006) doi:10.1088/1126-6708/2006/08/045 [hep-th/0605073].
- [13] A. Lewkowycz and J. Maldacena, “Generalized gravitational entropy,” *JHEP* **1308**, 090 (2013) doi:10.1007/JHEP08(2013)090 [arXiv:1304.4926 [hep-th]].
- [14] V. E. Hubeny, M. Rangamani and T. Takayanagi, “A Covariant holographic entanglement entropy proposal,” *JHEP* **0707**, 062 (2007) doi:10.1088/1126-6708/2007/07/062 [arXiv:0705.0016 [hep-th]].
- [15] X. Dong, “Holographic Entanglement Entropy for General Higher Derivative Gravity,” *JHEP* **1401**, 044 (2014) doi:10.1007/JHEP01(2014)044 [arXiv:1310.5713 [hep-th]].
- [16] V. E. Hubeny, H. Maxfield, M. Rangamani and E. Tonni, “Holographic entanglement plateaux,” *JHEP* **1308**, 092 (2013) doi:10.1007/JHEP08(2013)092 [arXiv:1306.4004 [hep-th]].

- [17] V. E. Hubeny and H. Maxfield, “Holographic probes of collapsing black holes,” JHEP **1403**, 097 (2014) doi:10.1007/JHEP03(2014)097 [arXiv:1312.6887 [hep-th]].
- [18] K. Narayan, “Extremal surfaces in de Sitter spacetime,” Phys. Rev. D **91**, no. 12, 126011 (2015) doi:10.1103/PhysRevD.91.126011 [arXiv:1501.03019 [hep-th]].
- [19] K. Narayan, “de Sitter space and extremal surfaces for spheres,” Phys. Lett. B **753**, 308 (2016) doi:10.1016/j.physletb.2015.12.019 [arXiv:1504.07430 [hep-th]].
- [20] N. Kim and J. Hun Lee, “Time-evolution of the holographic entanglement entropy and metric perturbationst,” J. Korean Phys. Soc. **69**, no. 4, 623 (2016) doi:10.3938/jkps.69.623 [arXiv:1512.02816 [hep-th]].
- [21] J. Bhattacharya, M. Nozaki, T. Takayanagi and T. Ugajin, “Thermodynamical Property of Entanglement Entropy for Excited States,” Phys. Rev. Lett. **110**, no. 9, 091602 (2013) doi:10.1103/PhysRevLett.110.091602 [arXiv:1212.1164 [hep-th]].
- [22] D. Momeni, M. Faizal, S. Bahamonde and R. Myrzakulov, Phys. Lett. B **762**, 276 (2016) doi:10.1016/j.physletb.2016.09.036 [arXiv:1610.01542 [hep-th]].